A transition from Kelvin–Helmholtz instabilities to propagating wave instabilities

François Lott
Laboratoire de Météorologie Dynamique du C. N. R. S., Ecole Polytechnique, 91128 Palaiseau Cedex, France

Hennie Kelder
Royal Netherlands Meteorological Institute, P.O. Box 201, 3730 AE De Bilt, The Netherlands

Hector Teitelbaum
Laboratoire de Météorologie Dynamique du C. N. R. S., Ecole Polytechnique, 91128 Palaiseau Cedex, France

(Received 29 January 1992; accepted 26 May 1992)

The object of this paper is to study the linear stability of an unbounded stably stratified shear layer in an inviscid, Boussinesq fluid. The flow is modeled by the velocity and buoyancy frequency profiles: $U=U_0\tanh(z/d)$ and $N^2=N_1^2+N_2^2\,|\tanh(z/d)|^\alpha$, where $\alpha>0$. It represents a shear layer which has already been mixed, to a certain extent, since the stratification is smaller inside the shear layer than outside. This flow can generate propagating wave instabilities if the layer of less static stability is sufficiently broad (i.e., α sufficiently large) as compared to the layer of large velocity shear: when $\alpha<2$, the flow only generates Kelvin–Helmholtz instabilities; when $\alpha>2$, the flow generates both Kelvin–Helmholtz and propagating wave instabilities. In three specific cases ($\alpha=0,2,4$), the neutral modes are derived systematically using an analytical transform of the Taylor–Goldstein equation into the hypergeometric equation. Furthermore, the neutral modes, associated to propagating wave instabilities, correspond to gravity waves with infinite critical level reflection and transmission (i.e., resonant overreflection). It is to be noted that resonant overreflection is possible in the present model as long as the minimum Richardson number of the flow is smaller than 0.25. In the conclusion, the importance of the results obtained is discussed, in relation with the spontaneous generation of gravity waves in a stratified shear layer.

I. INTRODUCTION

For the last 20 years, the reflection and the transmission of an internal gravity wave that is incident upon a stratified shear layer has been studied extensively. In a well-known paper on this subject, Booker and Bretherton[1] have shown that an incident wave is absorbed when the Richardson number at the critical level is larger than 0.25. When it is smaller than 0.25, overreflection can occur (i.e., the reflection coefficient of an incident wave is larger than 1) (Jones,[2] McKenzie,[3] Eltayeb and McKenzie,[4] and Acheson[5]). Furthermore, Miles[6] and Howard[7] have shown that the flow is stable when the minimum Richardson number is larger than 0.25; instabilities can arise when the minimum Richardson number is smaller than 0.25 (Drazin[8]). The fact that the behavior of both instabilities and gravity waves is indicated by the Richardson number, has led many authors to investigate the connection between unstable modes and overreflection (Lalas and Einaudi,[9] Davis and Peltier,[10] and Rosenthal and Lindzen[11]). An overreflected gravity wave can lead to an instability when it is reflected back toward its critical level by a rigid wall (or by a turning point beyond which the wave is evanescent). This "overreflection hypothesis" applies to very different types of instabilities in geophysical flows (Lindzen[12]). As noted by Smyth and Peltier,[13] it sometimes fails to explain the existence of unstable Kelvin–Helmholtz modes in Hölmböe-type flow when the Richardson number at the critical level is larger than 0.25. A complementary idea of this "overreflection hypothesis" is that of propagating wave instabilities where gravity waves are spontaneously emitted by the stratified shear layer, without being reflected back toward it. The neutral modes associated with these instabilities correspond to gravity waves with infinite reflection and transmission coefficients at the critical level. Using the terminology often seen in the literature, we shall name this phenomenon resonant overreflection. Note that this terminology is sometimes used for instabilities whose dynamic is related to the aforementioned "overreflection hypothesis" (Davis and Peltier[10]). In this paper, this "overreflection hypothesis" is not examined.

Most of the studies of linear resonant overreflection of gravity waves assume that the minimum Richardson number, J_1, is zero at the critical level. This often results from the use of discontinuous wind profile (the so-called vortex sheet) (McKenzie,[3] Grimshaw,[14] Lindzen,[15] and McIntyre and Weissman[16]). In continuous wind profiles, this results when the buoyancy frequency vanishes at the critical level (Grimshaw,[17] Lindzen and Barker,[18] and Lott and Teitelbaum[19]). In the linear picture of resonant overreflection, an instability provokes a disturbance at the shear layer, and this disturbance has a real phase speed and an horizontal wave number which equal those of gravity waves that propagate vertically outside of the shear layer. We can therefore presume that resonant overreflection is

 0899-8213/92/091990-08$04.00

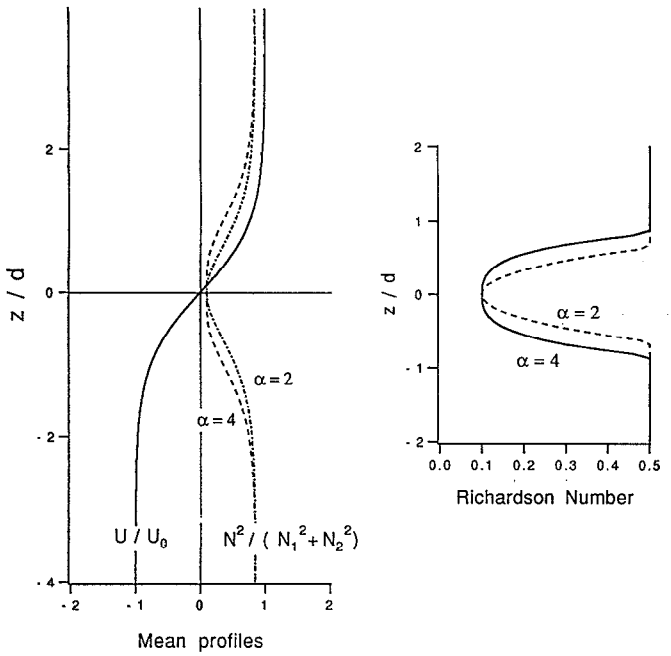

FIG. 1. Definition diagram for the velocity and stratification profiles.

favored when the stratification is smaller inside the shear layer than outside. On the one hand, inside the shear layer the static stability is small, so that the flow generates Kelvin–Helmholtz instabilities when the minimum Richardson number, J_1, is smaller than 0.25. On the other hand, the large stratification outside of the shear layer favors the onset of vertically propagating gravity waves. Troitskaya and Fabrikant[20] have shown that in a mean flow configuration such as this, resonant overreflection is possible for long gravity waves, even when the minimum Richardson number is not zero at the critical level. In these circumstances, when propagating wave instabilities occur, there must be a transition from Kelvin–Helmholtz instabilities (which are generally "trapped" at the shear layer) to the propagating wave instabilities. The purpose of this paper is to describe such a transition.

In this paper, the basic flow is

$$U=U_0\tanh(z/d),\quad N^2=N_1^2+N_2^2|\tanh(z/d)|^{\alpha},\quad (1)$$

where $\alpha>0$. These profiles are represented in Fig. 1, for $\alpha=2$ and 4. It represents a flow in which the depth of the layer of less static stability and the depth of the shear layer are different: when the parameter α increases, the depth of the layer of small stratification increases as compared to the depth of the shear layer. The fluid is incompressible, inviscid, and Boussinesq. Furthermore, we are studying unstable modes which admit a critical level at the inflection point of the wind profile. In fact, we know that unstable modes with nonzero real phase velocity (the so-called Hölmböe modes) cannot occur in this flow since the buoyancy frequency and the Richardson number are minima at $z=0$. This configuration is opposite to Hölmböe's, in which the buoyancy frequency and the Richardson number vanish outside of the shear layer, and where unstable modes with nonzero phase velocity can exist (Smyth and Peltier[13]). There are advantages of studying unstable modes in the flow defined by (1). First, when the profiles are smooth, the reflections occurring at the knees of piecewise linear profile (Jones[2] and Eltayeb and McKenzie[4]), are suppressed. Second, the modes found analytically in such a profile can serve as benchmarks for finite-difference numerical models calculating the temporal evolution of a free shear layer. Finally, the study of this type of profile allows a generalization of the Drazin,[8] Menkes,[21] and Van Duin and Kelder[22] analytical studies of neutral modes in profile (1) with $N_2^2=0$, and of the Lott and Teitelbaum[19] analytical study of resonant overreflection in profile (1) with $N_1^2=0$. In this paper, the determination of unstable modes is done analytically and numerically. When $\alpha=0$, 2, and 4, the neutral modes are calculated by transforming the wave equation into the hypergeometric equation. The determination of the unstable modes and the estimation of their influence on the background flow are done numerically by solving the wave equation using the method of Burlish and Stoer[23] adapted in Teitelbaum *et al.*[24] This model is also used to determine the neutral modes in profile (1) when $\alpha\neq0$, 2, and 4.

II. STATEMENT OF THE PROBLEM

The propagation of internal gravity waves is governed by the Synge–Taylor–Goldstein equation:

$$w_{zz}+\left(\frac{N^2}{(U-c)^2}-\frac{U_{zz}}{(U-c)}-k^2\right)w=0,\quad (2)$$

where w is related to the vertical velocity w' by,

$$w'(x,z,t)=\mathrm{Real}\{w(z)\exp[ik(x-ct)]\},$$

k and c being the horizontal wave number and the phase velocity of the disturbance, respectively. Assuming that U and N^2 are given by (1), and introducing the transformation of the independent variable, z,

$$r=s^2=[\tanh(z/d)]^2,$$

Eq. (2), for a neutral mode with zero real phase velocity, becomes

$$w_{rr}+\left(\frac{1}{2r}-\frac{1}{1-r}\right)w_r+\left(\frac{J_1+J_2r^{\alpha/2}}{4r^2(1-r)^2}+\frac{1}{2r(1-r)}-\frac{k^2d^2}{4r(1-r)^2}\right)w=0,\quad (3)$$

where $J_1=N_1^2d^2/U_0^2$ is the minimum Richardson number and $J_2=N_2^2d^2/U_0^2$ is a "pseudo" Richardson number characterizing the stratification outside of the shear layer. Equation (3) has three singularities at $r=0$, 1, and ∞. These singularities are regular when $\alpha=0$, 2, and 4 and therefore Eq. (3) can be solved analytically. The singular point $r=0$ is of particular interest since it separates the upper and lower half-plane: the solution relative to this point has to be made single valued. This is usually done by introducing a small dissipation (Booker and Bretherton[1]). In this case, the argument of $U-c$ in Eq. (2) passes from

0 to $-\pi$ when z passes from $+\infty$ to $-\infty$. Then, the choice of the correct branch in the complex plane is equivalent to write, $s=\exp(-i\pi)\,|s|$, when $s<0$.

The inviscid boundary conditions also need to be described. For large values of $|z|$, Eq. (2) writes,

$$w_{zz}+\left(\frac{N_1^2+N_2^2}{U_0^2}-k^2\right)w=0. \tag{4}$$

When $-\lambda^2=J_1+J_2-k^2d^2<0$, the neutral solutions of (2), outside of the shear layer, are nonpropagating evanescent modes. In this case, the boundary conditions simply require that the vertical velocity vanishes at infinity:

$$w\approx A^{\pm}\exp(-\lambda|z/d|), \quad \text{for } z=\pm\infty. \tag{5}$$

According to (4), when $m^2=J_1+J_2-k^2d^2>0$, the neutral modes are propagating gravity waves on both sides of the shear layer. In this case, an incident gravity wave forced at $z=-\infty$ arrives at the shear layer. It gives rise to a reflected wave below the shear layer and to a transmitted wave above. When the incident wave is normalized to unity, the solution of (2) below the shear layer is

$$w\approx\exp(+imz/d)+R\exp(-imz/d). \tag{6a}$$

Above the shear layer, the solution of (2) takes the form

$$w\approx T\exp(-imz/d), \tag{6b}$$

R and T being the amplitude of the reflected and transmitted wave, respectively. Thus (6a) and (6b) are boundary conditions to be imposed on the solution of (2). In this case a neutral mode exists when the shear layer emits spontaneously vertically propagating gravity waves. This is equivalent to the resonant overreflection condition:

$$|R|=|T|=\infty.$$

III. SOLUTION FOR $\alpha=2$

A. Trapped modes: $J_1+J_2-k^2d^2<0$

Equation (3) has three regular singular points of which the exponent pairs are real,

$$r=0, \quad \alpha_2^1=[\tfrac{1}{2}\pm(\tfrac{1}{4}-J_1)^{1/2}]/2, \tag{7a}$$

$$r=1, \quad \gamma_2^1=\pm(k^2d^2-J_1-J_2)^{1/2}/2, \tag{7b}$$

$$r=\infty, \quad \beta_2^1=\begin{cases}1\\-1/2\end{cases}. \tag{7c}$$

Then, Eq. (3) can be transformed into the hypergeometric equation (Olver[25]) by considering the new variable,

$$w=r^{\alpha_1}(1-r)^{\gamma_1}W,$$

and becomes

$$W_{rr}+\left(\frac{1-\alpha_1-\alpha_2}{r}-\frac{1-\gamma_1-\gamma_2}{r-1}\right)W_r$$
$$+\frac{(\alpha_1+\beta_1+\gamma_1)(\alpha_1+\beta_2+\gamma_1)}{r(r-1)}W=0. \tag{8}$$

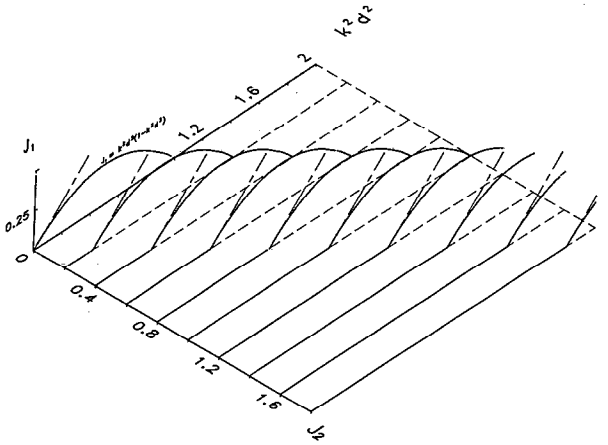

FIG. 2. Neutral curves and separation line ($J_1=k^2d^2-J_2$) in the (J_1,k^2d^2) plane for ten values of J_2, $\alpha=2$.

The boundary conditions (5) are now that W is regular at $r=0$, 1. As in Drazin,[8] Eq. (8) has a simple solution, $W=A=cte$, when the exponents satisfy

$$\alpha_1+\beta_2+\gamma_1=0 \tag{9a}$$

(equation $\alpha_1+\beta_1+\gamma_1=0$ has no solution). The same procedure, but changing α_1 into α_2 in the preceding transformation of Eq. (3), leads to a second simple solution when the exponents satisfy

$$\alpha_2+\beta_2+\gamma_1=0. \tag{9b}$$

These two relations lead to the condition:

$$J_1=(k^2d^2-J_2)(1-k^2d^2+J_2).$$

When $J_2=0$, we find again the relation of Drazin,[8]

$$J_1=k^2d^2(1-k^2d^2),$$

which delimitates in the (J_1, k^2d^2) plane, the domain within which the Kelvin–Helmholtz instabilities exist. Increasing J_2 (Fig. 2), and in the corresponding (J_1, k^2d^2) plane, this neutral curve is translated along the k^2d^2 axis with an unchanged shape. The constant of translation is J_2 and the neutral curve remains on the right-hand side of the line, $J_1=k^2d^2-J_2$.

B. Propagating modes: $J_1+J_2-k^2d^2>0$

Equation (3) is similarly reduced to the hypergeometric equation (8) (Van Duin and Kelder[22]), the exponents, γ_2^1, corresponding to the singular point $r=1$ are now imaginary:

$$r=1, \quad \gamma_2^1=\pm i(J_1+J_2-k^2d^2)^{1/2}/2.$$

The exponent pairs corresponding to $r=0$ and $r=\infty$ are unchanged [(7a) and (7c)]. With respect to the singularity $r=0$, the solution is given by

$$w(r)=r^{\alpha_1}(1-r)^{\gamma_1}[p_1W_1^0(r)+p_1W_2^0(r)], \tag{10}$$

with $W_1^0(r)=F(a,b;c;r)$ and $W_2^0(r)=r^{1-c}F(1+a-c, 1+b-;2-c;r)$.

The symbol F denotes the hypergeometric power series and,

$$a=\alpha_1+\beta_1+\gamma_1,$$

$$b=\alpha_1+\beta_2+\gamma_1,$$

$$c=1+\alpha_1-\alpha_2.$$

In the next development, the wave solution (10) is made single valued in the vicinity of $r=0$ and is rewritten with respect to the singularly $r=1$. Then, an equivalent form of (10) is found at $z=\pm\infty$ and the reflection and transmission coefficients are determined by comparing this equivalent form to (6a) and (6b). Such a procedure is carefully described in Van Duin and Kelder,[22] and the reader is referred to this paper for more details. Finally, the reflection and transmission coefficients can be expressed in terms of Γ functions:

$$R=\frac{-2iA_3A_1\sin(\pi p)}{A_3A_2\exp(-i\pi p)-A_1A_4\exp(+i\pi p)}, \tag{11a}$$

$$T=\frac{A_3A_2-A_1A_4}{A_3A_2\exp(-i\pi p)-A_1A_4\exp(+i\pi p)}, \tag{11b}$$

where

$$A_1=\frac{\Gamma(c)\Gamma(c-a-b)}{\Gamma(c-a)\Gamma(c-b)}, \quad A_2=\frac{\Gamma(c)\Gamma(a+b-c)}{\Gamma(a)\Gamma(b)},$$

$$A_3=\frac{\Gamma(2-c)\Gamma(c-a-b)}{\Gamma(1-a)\Gamma(1-b)},$$

$$A_4=\frac{\Gamma(2-c)\Gamma(a+b-c)}{\Gamma(1+a-c)\Gamma(1+b-c)},$$

and,

$$p=(0.25-J_1)^{1/2}.$$

We found that resonant overreflection only occurs when $J_1=0$, for all wave numbers corresponding to propagation wave: $k^2d^2\leqslant J_2$ (Fig. 2). This result is an extension of Van Duin and Kelder[22] who found resonant overreflection in the Drazin[8] profile [profile (1) with $J_2=0$] for infinitely long waves (i.e., $J_1=k^2d^2=0$). This also covers the results of Lott and Teitelbaum[19] who found resonant overreflection in profile (1) when the buoyancy frequency vanishes at the critical level, $N_1^2=J_1=0$. In this case, the neutral curve formed by those modes fits with the axis $J_1=0$ (Fig. 2). It does not delimitate a domain of instability in the (J_1, k^2d^2) plane. Furthermore, the neutral curves corresponding to the trapped modes found in Sec. III A, connect with the curves of resonant overreflection at the points ($J_1=0$; $k^2d^2=J_2$).

These results, added to those found in Sec. III A, show that when $\alpha=2$, and for a given value of J_2, the domain of instability in the (J_1,k^2d^2) plane, found by Drazin,[8] is translated along the k^2d^2 axis. The value of the constant of translation is J_2 and the unstable modes remain on the right-hand side of the curve, $J_1+J_2-k^2d^2=0$: no instability corresponds to propagating wave modes.

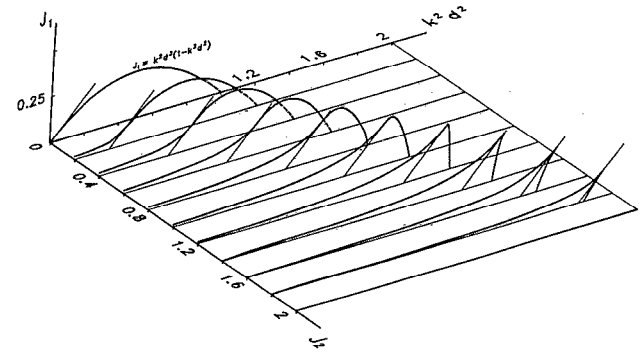

FIG. 3. Neutral curves and separation lines ($J_1=k^2d^2-J_2$) in the (J_1,k^2d^2) planes for 11 values of J_2, $\alpha=4$.

Furthermore, the onset of resonant overreflection when $J_1=0$ indicates that the configuration with $\alpha=2$ in profile (1) is a limit above which propagating wave instabilities exist. In fact, increasing α in the profile (1) destabilizes the shear layer because the depth of the layer where the buoyancy frequency and the Richardson number are close to their minimum value, N_1^2 and J_1, grows (Fig. 1). For $\alpha>2$ we have found that propagating wave instabilities occur, while for $\alpha<2$, such instabilities do not occur. Two examples can be treated analytically: $\alpha=0$ and 4. The configuration $\alpha=0$ can be simply reduced to the case studied by Drazin[8] and Van Duin and Kelder[22] since it corresponds to a profile of constant buoyancy frequency: no propagating wave instability occurs. The study of the configuration $\alpha=4$ provides interesting results.

IV. SOLUTION FOR $\alpha=4$

The analytical treatment of Eq. (2) is similar to that presented in Sec. III, except that the exponent pair corresponding to the singular point $r=\infty$ becomes

$$r=\infty, \quad \beta_2^1=[\tfrac{1}{2}\pm(\tfrac{9}{4}-J_2)^{1/2}]/2.$$

A. Trapped modes: $J_1+J_2-k^2d^2<0$

The neutral curves corresponding to the simple solution for which relations (9a) and (9b) are satisfied are represented in Fig. 3 for ten values of J_2. Contrary to the results found when $\alpha=2$, when $J=2$, when J_2 increases, the neutral curve corresponding to the trapped unstable modes is distorted compared to the Drazin[8] curve ($J_2=0$). Furthermore, when $J_2<2$ and when approaching the separation line $J_1+J_2-k^2d^2=0$, in the (J_1,k^2d^2) plane, the value of J_1 for which a neutral mode exists does not go to zero. Note also that when $J_2>2$ no instability occurs, while for $\alpha=2$ unstable modes exist.

B. Propagating modes: $J_1+J_2-k^2d^2>0$

Figure 3 also represents the locus of resonant overreflection in the (J_1, J_2, k^2d^2) space, R and T being determined by the formulas (11a) and (11b). Furthermore, we verify numerically that above the curve of resonant over-

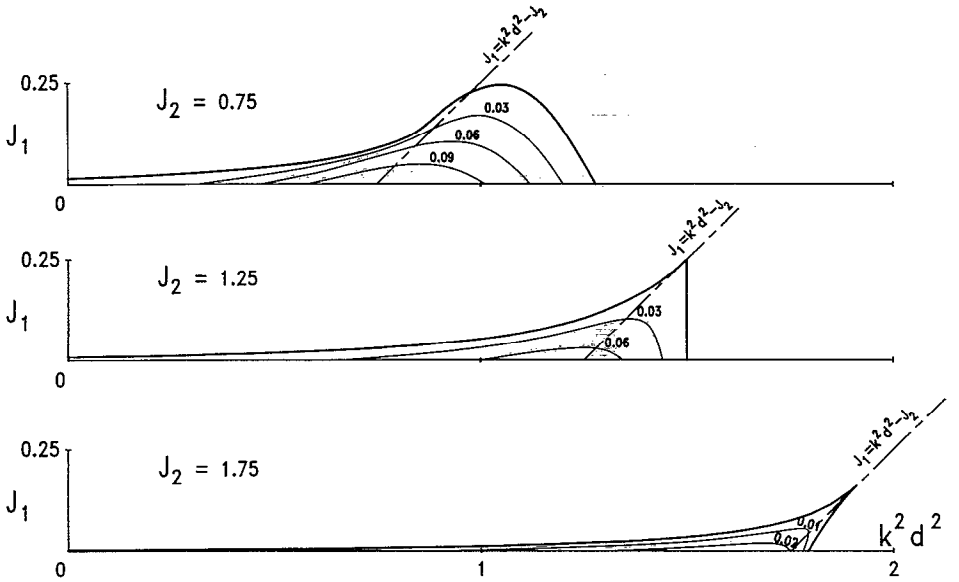

FIG. 4. Same as Fig. 2, for three values of J_2. The curves of constant normalized growth rates $\sigma = kd$ Im (c/U_0) are also represented.

reflection, unstable modes exist (Fig. 4). First, we found that as long as $0 < J_2 < 2$, resonant overreflection can occur for $J_1 \neq 0$. The case $J_1 = 0$ was treated by Lott and Teitelbaum[19] who found resonant overreflection when $J_2 = 2$ and unstable modes when $J_2 < 2$. Figure 3 also shows that, in the (J_1, k^2d^2) planes, the curves of neutral trapped modes connect to the curves of resonant overreflection through the separation plane $J_1 + J_2 - k^2d^2 = 0$. This connection corresponds to a transition from the Kelvin–Helmholtz instabilities to propagating wave instabilities.

As can be seen in Fig. 3, the nature of this transition in the (J_1, k^2d^2) plane, depends on whether J_2 is larger or smaller than 1.25. When $J_2 < 1.25$ the transition is smooth and when $1.25 < J_2 < 2$ it is sharp. When the transition is smooth the value of the minimum Richardson number J_1, for which a neutral mode occurs, decreases rapidly when passing the separation plane from the "trapped modes" zone to the "propagating modes" zone. Figure 4 further shows that in a given mean flow configuration (i.e., J_1 and J_2 are fixed) the growth rate of propagating unstable modes is significantly lower than those of the trapped modes. Nevertheless, when J_2 increases, this situation starts to reverse and the maximum value of the minimum Richardson number, J_1, for which resonant overreflection occurs, becomes larger and larger: it approaches 0.25 when J_2 approaches the critical value 1.25. At the limit $J_2 = 1.25$, resonant overreflection occurs as long as $J_1 < 0.25$. When the transition is sharp, $2 > J_2 > 1.25$, the area for which propagating unstable modes occur becomes significantly larger than the area for which trapped unstable modes occur. In this case it is important to note that in a given mean flow configuration, the propagating unstable modes grow more rapidly than the trapped modes (Fig. 4). It can also be seen in Fig. 3 that the form of the neutral curve in the (J_1, k^2d^2) plane becomes sharp in the vicinity of the separation plane. This curve becomes narrower and sharper as J_2 approaches 2 (Fig. 3), the maximum value of the minimum Richardson number, J_1, below which unstable modes exist decreases when J_2 increases. It approaches 0 when J_2 approaches 2.

As noted earlier, the critical value of J_2, which separates smooth and sharp transitions, is of great interest. It separates configurations for which the most unstable modes are trapped to those where they are propagating. We have also found, solving numerically the Taylor–Goldstein equation (2) for different values of α, that this critical value of J_2 decreases when α increases. It means that when the depth of the layer of small static stability increases as compared to the depth of the shear layer, the generation of propagating wave instabilities is favored.

C. Wave-mean flow exchanges

In order to get better physical insights into the mechanisms driving both types of instabilities, it is convenient to consider their energy exchanges with the background flow, as well as the resulting mean flow distorsion. The linear theory, neglects this mean flow changes, and does not describe the time evolution of the different energy reservoirs. Nevertheless, it can provide information about the first steps of the nonlinear processes when the disturbance and the related mean flow distortions are very small. Defining the horizontal velocity $u'(x,z,t)$, and the buoyancy force $\varphi'(x,z,t)$ associated to the wave, the corresponding mean flow distortion, $\bar{u}(z,t)$ and $\bar{\varphi}(z,t)$, follow the equations

$$\frac{d\bar{u}}{dt} = -\frac{\partial \overline{u'w'}}{\partial z}, \tag{12a}$$

$$\frac{d\bar{\varphi}}{dt} = -\frac{\overline{\varphi'w'}}{\partial z}, \tag{12b}$$

where the overbar means $\overline{(\ )} = k/2\pi \int_0^{2\pi/k} dx$.

Here, $u'(x,z,t)$ and $\varphi'(x,z,t)$ are related to the vertical velocity $w'(x,z,t)$ by the relations

$$\{u',\varphi',w'\}=\text{Real}\{\{u,\varphi,w\}\exp[ik(x-ct)]\},$$

$$iku+\frac{\partial w}{\partial z}=0,$$

and

$$ik(U-c)\varphi+N^2w=0.$$

The wave mean flow exchanges also satisfy an energy closure close to that presented by Klassen and Peltier.[26] Without dissipative effects, it involves the following energy reservoirs:

$\bar{K}=\frac{1}{2}\langle\overline{u_T^2}\rangle$, the mean kinetic energy; $\bar{u}_T=U+\bar{u}$,

$K'=\frac{1}{2}\langle\overline{u'^2}+\overline{w'^2}\rangle$, the wave kinetic energy,

$\bar{P}=-\langle z\bar{\varphi}\rangle$, the mean potential energy,

where the brackets mean, $\langle(\ )\rangle=\int_{-\infty}^{+\infty}(\ )dz$.

Assuming that the eddy interaction terms are sufficiently small, third-order nonlinear terms can be neglected and the energetic balances can be written as

$$\frac{d\bar{K}}{dt}=-C(\bar{K},K'),$$

$$\frac{dK'}{dt}=+C(\bar{K},K')+C(\bar{P},K'),$$

$$\frac{d\bar{P}}{dt}=-C(\bar{P},K'),$$

where

$$C(\bar{K},K')=\left\langle U\frac{\partial\overline{u'w'}}{\partial z}\right\rangle, \tag{13a}$$

$$C(\bar{P},K')=-\left\langle z\frac{\partial\overline{\varphi'w'}}{\partial z}\right\rangle. \tag{13b}$$

Here, the notation $C(\alpha,\beta)$ denotes the conversion of energy from reservoir α to reservoir β. The relations (13a) and (13b) show that these energy transfers are mainly related to the divergence of the momentum and buoyancy fluxes (12a) and (12b) transported by the wave. Those forcings are represented in Fig. 5, for four different unstable modes, and for a given amplitude of the disturbance. According to expressions (12a) and (12b), it shows that whatever the nature of the mode considered (trapped or propagating), the instability tends to take the mean horizontal momentum and buoyancy from above the critical level and restore them below. According to expression (13a) and (13b), this naturally induces a positive (negative) transfer of kinetic (potential)energy from the mean flow toward the wave. These energy transfers are characteristics of Kelvin–Helmholtz instabilities in stratified flows. In fact, in order to grow, Kelvin–Helmholtz instabilities pick up kinetic energy to the mean flow from around the critical level. Nevertheless, part of this kinetic energy returns to the mean flow as potential energy instead

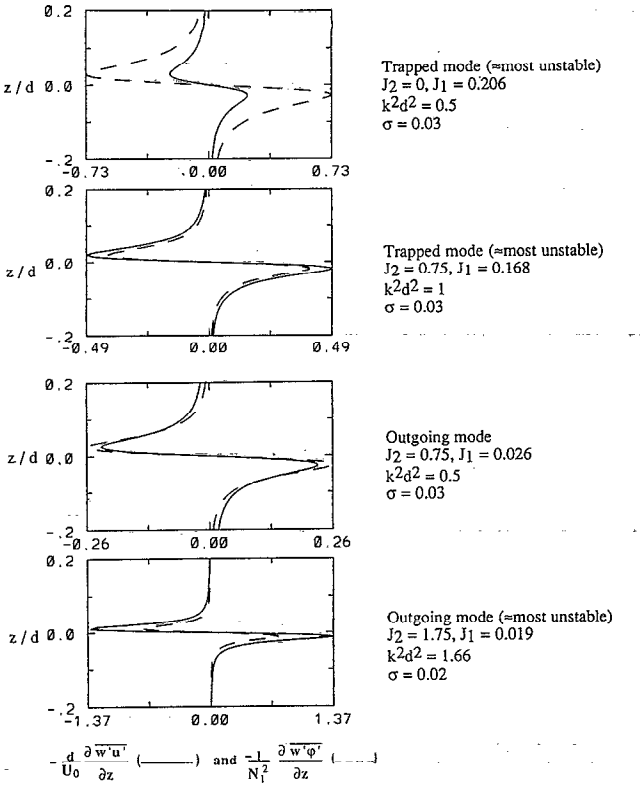

FIG. 5. Divergence of the vertical fluxes of horizontal momentum and buoyancy, for four different unstable modes; $\alpha=4$.

of contributing to the growth of the wave. This last effect is a natural consequence of the stabilizing influence of the background density stratification. Thus, from an energy point of view, the physics of the processes generating trapped instabilities and propagating wave instabilities are very similar. This is particularly evident in Figs. 5(b) and 5(c), where two unstable modes, existing in close mean flow configuration (α and J_2 are identical) and with similar growth rates, are compared. While these modes are very different outside of the shear layer [Fig. 5(b) corresponds to a trapped instability and Fig. 5(c) corresponds to a propagating instability], the shape of the momentum forcings are very close to each other. The same goes for the buoyancy forcings. These resemblances between the physical mechanisms driving both types of unstable modes support the basic assumption of this paper, i.e., that propagating wave modes are forced at the shear layer by a Kelvin–Helmholtz-type shear instability. This shear instability then supports wave radiation when the density stratification outside of the shear layer is sufficiently large.

Another interesting aspect of this analysis concerns the modification of the mean flow stability by the wave. The wave, by transporting downward momentum through the critical level, stabilizes the mean flow by decreasing its velocity shear. Nevertheless, since it also transports downward mean buoyancy, it destabilizes the mean flow by decreasing its stratification. The relative importance of these opposite effects can be measured by considering the temporal evolution of the mean flow stability (measured by the

Richardson number, Ri) around the critical level:

$$\left(\frac{\partial \mathrm{Ri}}{\partial t}\right)_{z\approx 0} \approx +J_1 \frac{\partial}{\partial t}\left(\frac{1}{N_1^2}\frac{\partial \bar{\varphi}}{\partial z} - 2\frac{d}{U_0}\frac{\partial \bar{u}}{\partial z}\right)$$

$$\approx -J_1 \frac{\partial}{\partial z}\left(\frac{1}{N_1^2}\frac{\partial \overline{w'\varphi'}}{\partial z} - 2\frac{d}{U_0}\frac{\partial \overline{w'u'}}{\partial z}\right).$$

This tendency can be estimated by comparing the slopes of the momentum and buoyancy fluxes divergence around the critical level in Fig. 5. When the mean stratification is initially uniform in the whole fluids [$J_2=0$, Fig. 5(a)], and for the most unstable mode occurring in a given mean flow configuration (here, for $J_1=0.206$), the amplitude of the fluxes is such that the mean flow is destabilized. It shows that in an initially uniformly stratified flow, the most unstable mode mixes the mean density more rapidly than it mixes the velocity. This leads to a more unstable flow in which stratification is smaller around the critical level than outside of the shear layer. Even if the resulting mean flow configuration is certainly very different from those studied here, in the vicinity of the critical level, it has some resemblance to cases studied where the stratification is smaller at the shear layer than outside. As was shown in Sec. IV B, such a configuration can favor the onset of propagating wave instabilities. Figure 5(c) shows that this type of instability, as well as the most unstable trapped instability which can occur in a mean flow configuration such as this [Fig. 5(b)], stabilizes the shear layer. This stabilization becomes very efficient when the most unstable mode is a propagating wave instability [Fig. 5(d)].

V. CONCLUSION

This study of the linear stability of an unbounded stratified shear layer has provided several new results. It has shown that resonant overreflection and propagating wave instabilities can exist for all values of the minimum Richardson number, J_1, smaller than 0.25, when the background profiles are continuous and smooth. Furthermore, the mean flow configuration used allows analytical solutions that are extensions of well known studies (e.g., Drazin[8]) of such layers. Energy analysis indicates that the physical mechanisms driving trapped modes and propagating modes are very similar. For those reasons, the radiating wave instability can be viewed as the linear excitation of propagating waves by a Kelvin–Helmholtz unstable mode existing at the shear layer. This mode becomes propagating because the stratification is large outside of the shear layer. This complements the "overreflection hypothesis" (Lindzen[11]) where overreflected waves give rise to instabilities. In some cases we also find that the most unstable modes correspond to propagating wave instabilities.

From a more general point of view, this study shows that the nature of the unstable modes which develop in a stratified shear layer strongly depend on the background density stratification. Furthermore, the case for which the density stratification is smaller inside the shear layer than outside is studied. The existence of this mean flow configuration in geophysical fluids is not usual. Nevertheless, when instabilities develop in a uniformly stratified shear layer (i.e., with N^2 constant), they trend to decrease both the velocity shear and the density stratification at the shear layer. As Churilov and Shukhman[27] have shown in the weakly nonlinear viscous case, at $\mathrm{Pr}>1$, and as it was shown in Sec. IV C in the inviscid case, these changes do not necessarily lead to a stabilization of the background flow. This reduction of the mean stratification at the shear layer is also found in the fully nonlinear two-dimensional case (Klaassen and Peltier[26]). Their results seem realistic, even if Winters and Riley[28] have shown that the critical level dynamics is certainly three dimensional, and that two-dimensional simulations filter convective unstable modes which can be predominant during the disturbance breakdown (Winters and D'Asaro[29]). Nevertheless, we can presume that the three-dimensional wave overturning also tends to homogenize the potential temperature profile. This study indicates that turbulent shear layers such as these can be propitious to the spontaneous generation of propagating gravity waves through resonant overreflection. In this context, another important result of this paper is that the onset of propagating modes is also related to the depth of the "mixed" area, where the stratification is small. In this study, this was indicated by the parameter α. When α increases, the depth of the layer of less static stability increases as compared to the shear layer, and the generation of propagating waves is favored. This study further shows that contrary to the primary instability which tends to destabilize the flow, this second instability stabilizes it very efficiently. For these reasons, we can presume that propagating unstable modes can play an important part in the late development of an unstable stratified shear layer.

The applicability of our results to shear layer problems is limited by the linear hypothesis adopted, their dynamics being essentially nonlinear. Nevertheless, we can expect that the generation of propagating waves will be efficient when the unstable modes, which mix the mean potential temperature, combine together through vortex pairing (Collins and Maslowe[30]) and excite longer propagating wave unstable modes, like those presented here. Another interesting problem would consist in forcing an incident gravity wave below an unstable stratified shear layer, where trapped instabilities develop and mix the potential temperature.

[1] J. R. Booker and F. B. Bretherton, "The critical layer for internal gravity waves in a shear flow," J. Fluid Mech. **27**, 513 (1967).
[2] W. L. Jones, "Reflection and stability of waves in stably stratified fluid with shear flow: A numerical study," J. Fluid Mech. **34**, 609 (1968).
[3] J. F. McKenzie, "Reflexion and amplification of acoustic gravity waves at a density and velocity discontinuity," J. Geophys. Res., 2915 (1972).
[4] I. A. Eltayeb and J. F. McKenzie, "Critical-level behavior and wave amplification of a gravity wave incident upon a shear layer," J. Fluid Mech., 661 (1975).
[5] D. J. Acheson, "On over-reflexion," J. Fluid Mech., 433 (1976).
[6] J. W. Miles, "On the stability of heterogeneous shear flows," J. Fluid Mech. **10**, 498 (1961).
[7] L. N. Howard, "Note on a paper of John W. Wiles," J. Fluid Mech. **10**, 509 (1961).
[8] P. G. Drazin, "The stability of a shear layer in an unbounded heterogeneous inviscid fluid," J. Fluid Mech. **4**, 214 (1958).

[9]D. P. Lalas and F. Einaudi, "On the characteristics of gravity waves generated by atmospheric shear layers," J. Atmos. Sci. **33**, 1248 (1976).
[10]P. A. Davis and W. R. Peltier, "Some characteristics of the Kelvin Helmholtz and overreflection modes of shear flow and of their interaction through vortex pairing," J. Atmos. Sci. **36**, 2394 (1980).
[11]A. J. Rosenthal and R. S. Lindzen, "Instabilities in a stratified fluid having one critical level. Part II: Explanation of gravity wave instabilities using the concept of overreflection," J. Atmos. Sci. **40**, 521 (1983).
[12]R. S. Lindzen, "Instability of plane parallel shear flow (toward a mechanistic picture of how it works)," Pageoph. **126**, 103 (1988).
[13]W. D. Smyth and W. R. Peltier, "The transition between Kelvin Helmholtz and Holmboe instability: An investigation of the overreflection hypothesis," J. Atmos. Sci. **46**, 3698 (1989).
[14]R. H. J. Grimshaw, "On resonant over-reflexion of internal gravity waves from a Helmholtz velocity profile," J. Fluid. Mech. **90**, 161 (1979).
[15]R. S. Lindzen, "Stability of a Helmholtz velocity profile in a continuously stratified inviscid Boussinesq fluid-applications to clear air turbulence," J. Atmos. Sci. **31**, 1190 (1974).
[16]M. E. McIntyre and M. A. Weissman, "On radiating instabilities and resonant overreflection," J. Atmos. Sci. **35**, 1190 (1978).
[17]R. H. J. Grimshaw, "Resonant over-reflection of internal gravity waves from a thin shear layer," J. Fluid Mech. **109**, 349 (1981).
[18]R. S. Lindzen and J. W. Barker, "Instability and wave overreflection in stably stratified shear flow," J. Fluid Mech. **151**, 189 (1985).
[19]F. Lott and H. Teitelbaum, "Influence of dissipation on gravity waves propagating through a shear layer and on instabilities: Validity of the linear approximation," Ann. Geophys. **8**, 37 (1990).
[20]Y. I. Troitskaya and A. L. Fabrikant, "Resonant amplification of internal gravity waves in shear flow," Izv. Vyssh, Uchebn. Zaved. Radiofiz. **32**, 1221 (1989).
[21]J. Menkes, "On the stability of a heterogeneous shear layer subject to a body force," J. Fluid Mech. **11**, 284 (1961).
[22]C. A. Van Duin and H. Kelder, "Reflection properties of internal gravity waves incident upon a hyperbolic tangent shear layer," J. Fluid Mech. **120**, 505 (1982).
[23]R. Burlish and J. Stoer, "Numerical treatment of ordinary differential equations by extrapolation methods," Num. Math. **8**, 1 (1966).
[24]H. Teitelbaum, H. Kelder, and C. A. Van Duin, "Propagation of internal gravity waves in a rotating fluid with shear flow," J. Atmos. Terrest. Phys. **49**, 413 (1987).
[25]F. W. J. Olver *Asymptotics and Special Functions,* Computer Science and Applied Mathematics (Academic, New York, 1974).
[26]G. P. Klaassen and W. R. Peltier, "Evolution of finite amplitude Kelvin Helmholtz billows in two spatial dimensions," J. Atmos. Sci. **42**, 1321 (1985).
[27]S. M. Churilov and I. G. Shukhman, "Nonlinear stability of a stratified shear flow: A viscous critical layer," J. Fluid Mech. **180**, 1 (1987).
[28]K. B. Winters and J. J. Riley, "Instability of internal waves near a critical level," Dyn. Atmos. Oceans **16**, 249 (1992).
[29]K. B. Winters and E. A. D'Asaro, "Two dimensional instability of finite amplitude internal gravity wave packets near a critical level," J. Geophys. Res. **94**, 12709 (1989).
[30]D. A. Collins and S. A. Maslowe, "Vortex pairing and resonant wave interactions in a stratified free shear layer," J. Fluid Mech. **191**, 465 (1988).